J Mater Sci (2009) 44:931–938
DOI 10.1007/s10853-008-3189-6

Macroporous alumina monoliths prepared by filling polymer foams with alumina hydrosols

Yuan Zhang · Hao Liang · Cun Yu Zhao · Yuan Liu

Received: 16 October 2008 / Accepted: 11 December 2008 / Published online: 31 December 2008

Abstract Macroporous alumina monoliths have been prepared for the first time by filling polystyrene foam templates with alumina hydrosols which were prepared from pseudo-boehmite. Polystyrene foam templates were obtained by polymerization in highly concentrated water-in-oil (W/O) emulsions. The organic templates were subsequently removed by calcination. The effects of filling times of the alumina hydrosols, calcination temperature, and CTAB surfactant addition in the hydrosols on the properties of the monolith have been investigated. TG, FT-IR, SEM, TEM, N_2 adsorption–desorption, and XRD techniques were used for characterization. The so prepared monoliths are the replicas of the polystyrene foams and are characterized with hierarchically porous structure. The macropores are interconnected and the macropore walls contain many meso and/or micropores. The hierarchically macro-meso-microporous structure can be controlled and tailored by adjusting the preparation conditions stated above and by addition of surfactant, and the organic components can be eliminated by high temperature calcination. When the calcination temperatures are 600 °C and 900 °C, the γ-Al_2O_3 phases are obtained, with S_{BET} of 228 and 85 m^2 g^{-1}, respectively. When calcined at 1100 °C, the alumina monolith presents a single θ-Al_2O_3 phase with S_{BET} of 80 m^2 g^{-1}. The 1300 °C calcined sample takes on the single α-Al_2O_3 phase with S_{BET} of 5 m^2 g^{-1} and compressive strength of 3.1 MPa.

Electronic supplementary material The online version of this article (doi:10.1007/s10853-008-3189-6) contains supplementary material, which is available to authorized users.

Y. Zhang · H. Liang · C. Y. Zhao · Y. Liu (✉)
Tianjin Key Laboratory of Applied Catalysis Science and Engineering, Department of Catalysis Science and Technology, School of Chemical Engineering and Technology, Tianjin University, Tianjin 300072, China
e-mail: yuanliu@tju.edu.cn

Y. Zhang
e-mail: zhangyuan2006a@tju.ed.cn

Introduction

Hierarchically porous materials with multiple-scale porous structure have attracted great attention recently due to their potential applications in various fields, such as heterogeneous catalysts [1, 2], chemical separations [3], electrode materials [4]. As for preparing hierarchically porous materials, the macropores are fabricated by emulsion templating [5, 6] or colloidal crystal templating [7, 8]. To create meso-macroporous structures, the surfactants are also used [7–9].

Many compounds have been made in monolithic shape with hierarchical pores, such as silica [10–12], titania [10, 13], zirconia [10], carbon [3, 14–16], and polymer [17, 18]. These micro-meso-macroporous monoliths are generally prepared with polymer template method [10–13] including the following steps: (1) to prepare macroporous organic foam with a certain shape, (2) to fill the organic foam with precursor sol, (3) to remove the template by calcination or etching. The resultant monoliths are the replica of the polymer foams both in microscopic and macroscopic scales, although volume shrinkage takes place to some extent. The shape of the templates can be controlled and molded with mold [10], and the macropore size can be adjusted by changing the volume fraction of the dispersed phase [13]. Theoretically speaking, if the appropriate template and precursor have been chosen, macroporous monolith of various compounds can be obtained in any

shape with adjustable macropore sizes. This preparation method has attractive advantages, such as pore structure controllable and shape moldable as stated above. However no reports can be found for preparing alumina monolith with hierarchically porous structure by using this method up to now.

Alumina is a very important inorganic material owning to its thermal, chemical, and mechanical stability, and the hierarchically porous alumina should be an attractive material which can be potentially used as catalyst supports, adsorbents, ion-exchange materials, membrane substrates, etc.[19–21]. Several reports on porous alumina monolith preparation can be found (not by using the template method). Fujita and co-workers prepared macro-mesoporous alumina monolith [22, 23] and silica–alumina monolith [24] by using a sol-gel method combined with phase separation. Yan et al. prepared bimodal porous alumina foam with pore size in mm level by sponge-pore-former method [25, 26].

In this work, macroporous alumina monoliths have been made with the template method by filling polystyrene foam templates with alumina hydrosols, and it is known that alumina hydrosol is facile to be made [27]. This method possesses the advantages of the template method for porous material preparation.

Experimental

Materials

The monomer styrene came from Tianjin Reagent Co. (China), and the crosslinking agent divinylbenzene (DVB) from Alfa Aesar (UK). The initiator 2,2′-azobisisobutyronitrile (AIBN) and the nonionic surfactant Span 80 (sorbitan monooleate) were purchased from Tianjin Jiang Tian Reagent Co. (China). Other chemicals, cetyltrimethylammonium bromide (CTAB) and nitric acid were also purchased from Tianjin Jiang Tian Reagent Co. (China). Pseudo-boehmite was provided by Zibo Sen Chi Chemical Co. (China).

Preparation of polystyrene template

The polystyrene foams were obtained by polymerization of styrene in highly concentrated water-in-oil (W/O) emulsions. Both of the monomer styrene and the crosslink agent DVB were washed with 0.2 mol L^{-1} NaOH and then with deionized water to remove inhibitors. Styrene (2.0 g), DVB (0.5 g), AIBN (20 mg), and Span 80 (90 mg) were introduced into a flask to form a homogeneous phase. Then water was added dropwise into the homogeneous phase with a syringe at room temperature under stirring, until the volume fraction of the water reached 0.82, thus the highly concentrated water-in-oil (W/O) emulsion was generated. The emulsion was put in a glass mold (i.d. 7 mm, length 100 mm) which was then sealed with a plug and maintained at 60 °C for 24 h, during which time polymerization of styrene occurred. The wet polystyrene monoliths were removed from the molds by carefully breaking the glass containers, and then dried at 60 °C for 24 h, to obtain polystyrene monolithic templates. The template foams were divided into short cylinders with a knife.

Preparation of macroporous alumina monolith

Macroporous alumina monoliths were prepared by imbibing macroporous polystyrene foams with the alumina hydrosol. The hydrosols were prepared as follows: 4 g pseudo-boehmite was added into 60 mL deionized water under stirring. After aging for 1 h, 1 mol L^{-1} HNO_3 was dropped into the system with a ratio of $n(Al^{3+}):n(H^+) = 1:0.03$. The translucent alumina hydrosol was obtained by aging it for 12 h under stirring at room temperature. The resultant alumina hydrosol was imbibed into the polystyrene template pores under vacuum of 0.098 MPa, and then the coated template was dried at 60 °C for 12 h. The coating and drying procedures were repeated for several times. The coated templates were calcined in air at 600 °C for 4 h to obtain macroporous alumina monolith. The heating rate was 1 °C min^{-1}. Then the Al_2O_3 monolithic oxides were further calcined at 900 °C, 1100 °C, or 1300 °C for 2 h, respectively.

For preparing the meso-macroporous monoliths, CTAB was added into the alumina hydrosol before aging. After filling and drying, the composites were calcined in air at 600 °C for 4 h.

Characterization

Thermo gravimetric analysis was carried out on a Perkin-Elmer Pyris TG instrument at a dry-air atmosphere with a heating rate of 10 °C min^{-1}.

Powder X-ray diffraction (XRD) patterns of the samples were recorded on Rigaku D/max 2500v/pc X-ray diffractometer in order to identify the phases presented in the samples and to calculate the crystal sizes. Copper Kα radiation ($\lambda = 0.15406$ nm) was used with a power setting of 40 kV and 100 mA. (Scan rate = 5° min^{-1}).

Fourier transformed infrared (FT-IR) spectra of the samples were measured by NICOLET Nexus FT-IR Spectrometer working in the wave number range of 4000–400 cm^{-1} with sample prepared by KBr method, where the sample to KBr ratio was 1:100.

Photographs of the monoliths were taken on an Olympus μ7000 digital camera.

Scanning electron microscopy (SEM) tests were performed on a Philips XL-30ESEM microscope with Au-sputtered specimen operated at 15 keV to observe the macroporous structure of the samples.

Transmission electron microscopy (TEM) pictures were obtained on a Technai G^2 F20 microscope operated at 200 kV. Samples were finely ground in an agate mortar to fine particles and dispersed ultrasonically in ethanol. The well dispersed samples were deposited on a Cu grid covered by a holey carbon film for measurements.

Nitrogen adsorption and desorption isotherms were determined on a Quantachrome Quadrosorb SI apparatus at −196 °C. The specific surface areas were calculated by using BET method at the relative pressure range of 0.05–0.30, and the pore size distributions were calculated from the adsorption branch of the isotherm with BJH model.

The compressive strengths of the calcined samples were measured using Shimadzu DSS-25T universal testing machine fitted with flat steel plates closing with a circular head at a speed of 0.5 mm min^{-1}.

The density of the alumina monoliths were measured as follows: the mass of the alumina monoliths was measured by using an electronic balance (US, Ohaus, CP-153). The volume of the monoliths was tested by using a cylinder. Powder of SiC below 300 mesh was filled into the measuring cylinder, and the corresponding volume was V_1; then the alumina monolith was put into the SiC powder, and the corresponding volume was V_2. So, the volume of the alumina monolith was $V_2 - V_1$. The mass was divided by the volume, to obtain the density.

Results

Preparation of macroporous alumina monolith

To illustrate the variation in the preparation process of macroporous alumina monoliths, a sketch map is given (Fig. 1). During preparation of polystyrene (PS) template, water (dispersed phase) was added dropwise into the mixture of styrene and DVB (continuous phase). The surfactant should be located at the interface of the dispersed phase and the continuous phase. When the volume fraction of dispersed phase (φ) increased to 74.05%, the concentrated emulsion was formed and the droplets were close-packed with sphere shape. With further increase in φ, the droplets pressed each other to polyhedral shape and the continuous phase existed as liquid membrane. After polymerization and drying, template was obtained, with some surfactant left/adsorbed on the template surface. During filling step, alumina hydrosol filled into the hydrophobic template with the help of the surfactant residues. Finally, the template and surfactant were removed during calcination step, obtaining macroporous alumina monolith.

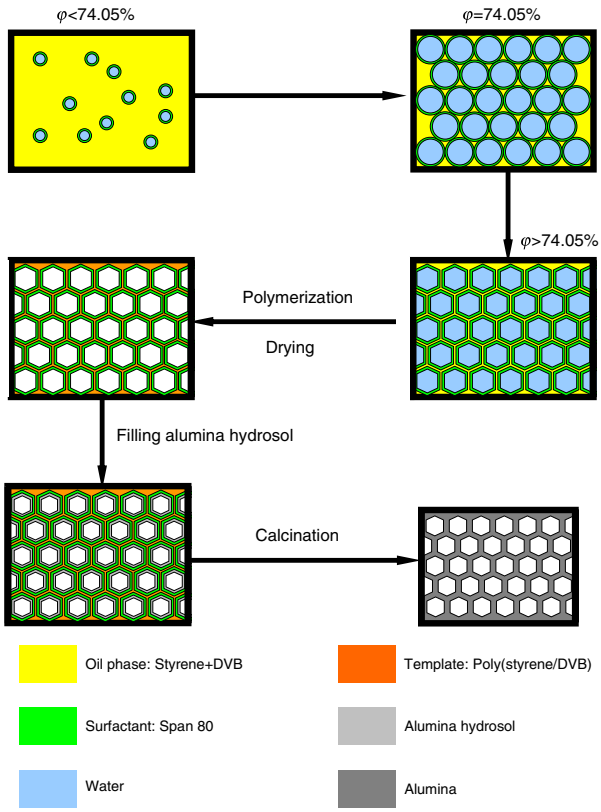

Fig. 1 Scheme of alumina macroporous monolith preparation

TG

Figure 2 is the TG curve of the Al_2O_3/PS composite, i.e., the polystyrene foam filled with alumina hydrosol after drying. From room temperature to 800 °C, there were four obvious weight loss stages: (1) before 100 °C, a weight loss of 8% was caused by the evaporation of surface water. Because the coated template was dried at 60 °C, there was still some water in the composite. (2) From 100 °C to 300 °C, a weight loss of 8% was due to the evaporation of structural water. (3) The large weight loss of 50% between 300 °C and 370 °C was attributed to the decomposition and combustion of the polystyrene template. (4) In the temperature range of 370 °C to 550 °C, a weight loss of 22% was owing to the transformation from γ-AlOOH to γ-Al_2O_3. As temperature was higher than 550 °C, no weight loss could be detected. The total weight loss was about 88%. From the FT-IR spectra (see S1 in supplementary information), the organic template residues were in trace level in the alumina monoliths calcined at 600 °C,

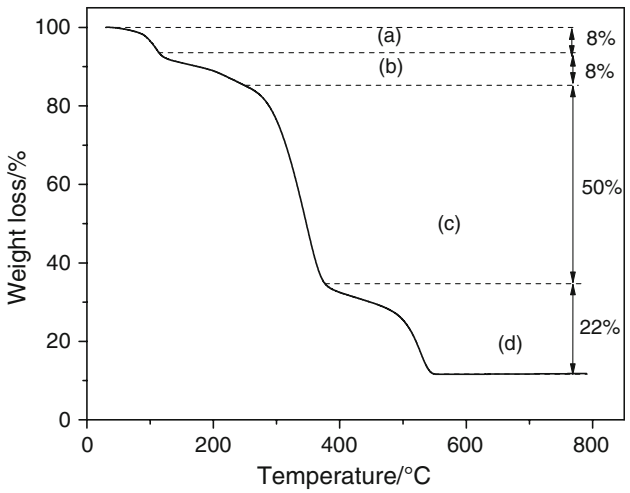

Fig. 2 TG curve of the Al_2O_3/PS composite. Weight loss of (a) surface water, (b) structural water, (c) PS decomposition, (d) transition from γ-AlOOH to γ-Al_2O_3

and no template was detected in the samples calcined at temperatures higher than 900 °C.

XRD

Figure 3 shows the XRD patterns of alumina monoliths calcined at different temperatures. It can be clearly seen that the monolith calcined at 600 °C (Fig. 3a) obtained a cubic γ-Al_2O_3 phase (JCPDS No. 10–0425). As calcination temperature did not exceed 900 °C, only crystallite γ-Al_2O_3 phase was observed. The crystallite sizes evaluated by Scherrer's equation were approximately 2.6 and 2.7 nm for the samples heat-treated at 600 and 900 °C, respectively. In 1100 °C calcined sample, monoclinic θ-Al_2O_3 phase (JCPDS No. 35–0121) appeared. When the

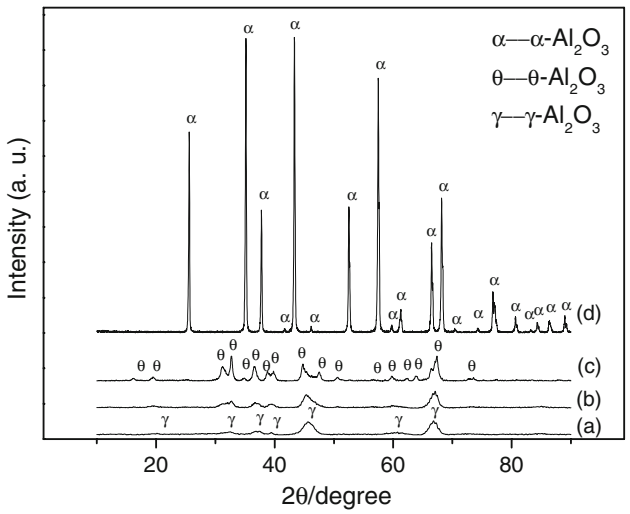

Fig. 3 XRD spectra of alumina monolith calcined at (a) 600 °C, (b) 900 °C, (c) 1100 °C, (d) 1300 °C

calcination temperature was raised to 1300 °C, a single phase of hexagonal α-Al_2O_3 (JCPDS No. 46–1212) was obtained with good crystallization. The results are consistent with the references [20, 25, 26, 28], which indicates that the template and the surfactant residues could hardly influence the crystal structure transformation of the alumina.

SEM images

Some photo pictures of the templates and the resultant meso-macroporous alumina monoliths are shown in S2 of the supplementary information. The shape and size of the macroporous polystyrene foams can be controlled by the shape and size of the container used for the styrene-emulsion polymerization. Cylindrical molds were used in this work. The shrinkage degree of alumina monoliths increases with the increase of calcination temperature. For the sample calcined at 1300 °C, the volume shrinkage is 40%. Aside from shrinkage, the bulk shape of the subsequent alumina monoliths did not change during the calcination. Thus, the bulk shape of alumina monoliths can be adjusted by changing the shape of the polymer foams.

SEM images of the templates and the alumina monoliths are shown in Fig. 4. Figure 4a is a representative picture of polystyrene foam monoliths, in which the macropores are in spherical shape with a diameter range of 10–50 μm. The spherical macropores are interconnected via windows with the diameters approximately 1–20 μm. The macropores were occupied by water during polymerization. After drying, the water vaporized, and left the interconnected macropores.

The microscopic appearance of macroporous alumina monolith (Fig. 4b) is the replica of corresponding polystyrene foam with shrinkage taken into account. The walls of the macropores of the alumina monolith consisted of two layers of alumina located on both sides of the formerly template walls, which can be seen from Fig. 4f. The wall thickness is about 0.3 μm.

The alumina monoliths calcined at 900 °C (Fig. 4c) and 1100 °C (Fig. 4d) present the similar macroporous structure to the sample calcined at 600 °C, excepting for that the windows between adjacent hollow balls become larger in the cases of 900 and 1100 °C calcination. The macropores in the samples consisted of the spherical pores and the windows between them. With increase in calcination temperature, the size of windows between the spherical pores increases, which should be due to the intensified sintering at the higher temperatures. When the calcination temperature is 1300 °C (Fig. 4e), the windows become larger, and the porous structure is much like that of ceramic foam or metallic foam, while the macropore size is in the

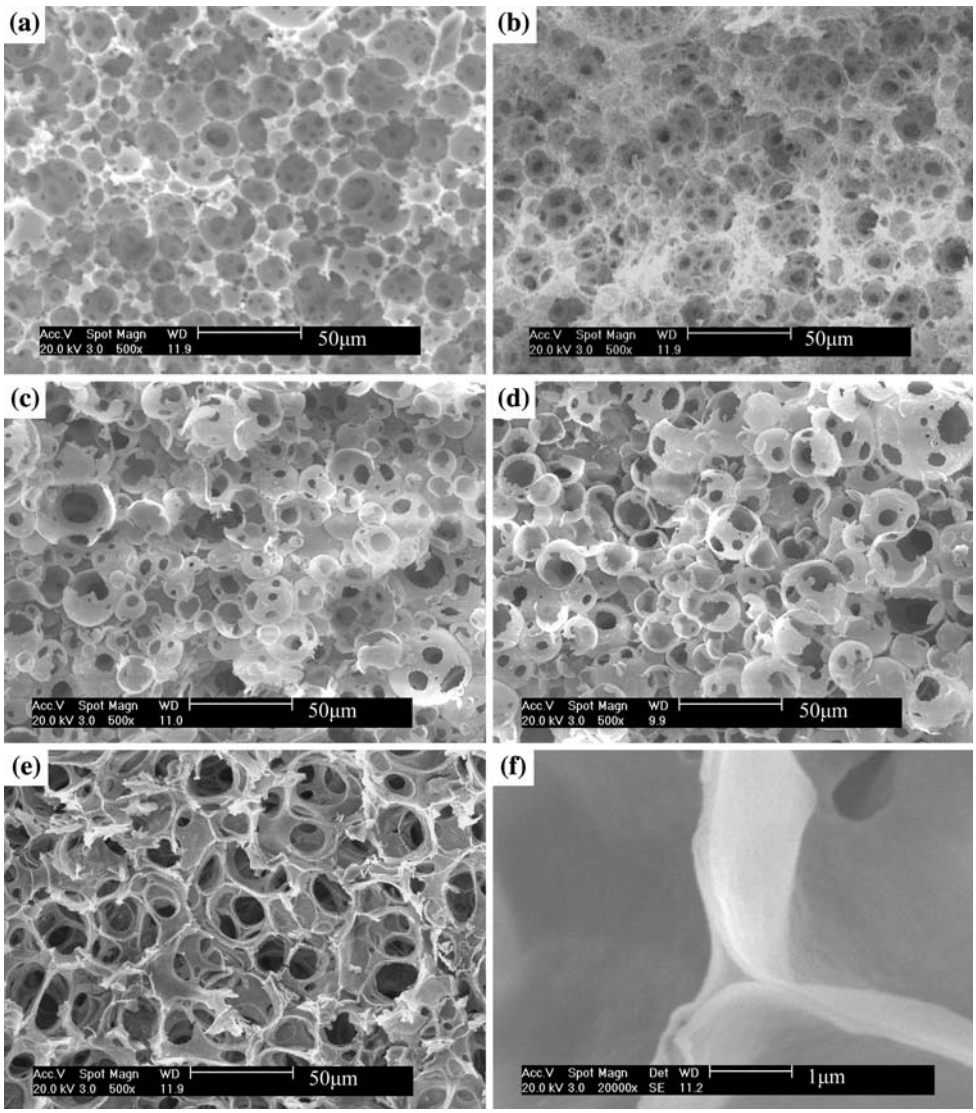

Fig. 4 SEM images of **a** polystyrene monolith; alumina monolith calcined at **b**, **f** 600 °C, **c** 900 °C, **d** 1100 °C, **e** 1300 °C. Scale bar: 50 μm for (**a**, **b**, **c**, **d**, **e**), and 1 μm for (**f**)

range of 20–30 μm which is much smaller than that of generally made ceramic and metallic foams [25, 26, 29].

As listed in Table 1, the compressive strength of alumina monoliths increases with the increase of calcination temperature. The corresponding stress–strain curves of different samples are shown in S3 of the supplementary information. As calcination temperature increases from 600 °C to 1300 °C, the mechanical strength increases from 0.123 MPa to 3.081 MPa. The alumina monolith calcined at 1300 °C exhibits the highest mechanical strength.

The macroscopic volume shrinkages and bulk densities of the alumina monoliths calcined at 600 °C are listed in Fig. 5. The volume shrinkages of the samples decrease with the increase in filling time. The density increases from 0.08 to 0.15 g cm^{-3} with the increase of the filling times. The shrinkage is nearly isotropic in the three dimensions;

Table 1 S_{BET}, pore size, and pore volume calculated from BJH model and strength data of alumina monoliths

Sample	With CTAB	BET surface area (m^2 g^{-1})	Pore diameter (nm)	Pore volume (cm^3 g^{-1})	Compressive strength (MPa)
600-Al_2O_3	No	228	2.2	0.190	0.123
600-Al_2O_3–C	Yes	251	2.2, 6.5	0.384	–
900-Al_2O_3	No	85	6.5	0.169	0.713
1100-Al_2O_3	No	80	5.6	0.168	0.759
1300-Al_2O_3	No	5	2.8	0.010	3.081

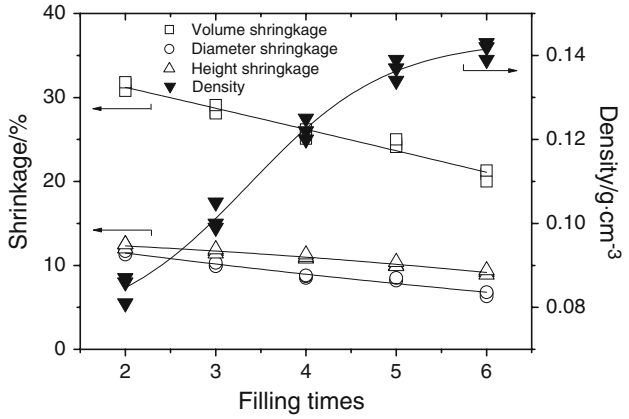

Fig. 5 Macroscopic volume shrinkages and bulk densities of the 600 °C calcined alumina monolith plotted with different filling times

the diameter shrinkage is a little smaller than the height shrinkage. The volume shrinkage is between 21% and 32% and both the diameter and height shrinkage are below 13%, which are much lower than those of silica monolith in Ref [10]. The shrinkage data given by Ref [10] are in one-dimensional length scale, for example, 25% in one-dimensional length scale is corresponding to about 58% of volume shrinkage in three-dimensional scale. It is hard to obtain the accurate data of the lower compressive strength due to the error bar limitation of the universal testing machine. So the compressive strength data of the 600 °C samples with different filling times were not included. Generally, the sample with higher density takes on the higher compressive strength.

N_2 adsorption–desorption

S_{BET}, pore size, and pore volume of the alumina monoliths calculated from BJH model are listed in Table 1. The specific surface areas and the pore volumes of the samples decrease with the increase of the calcination temperature. From 600 °C to 900 °C, the specific surface area decrease from 228 to 85 $m^2\ g^{-1}$. S_{BET} of the monolith calcined at 1100 °C for 4 h is 80 $m^2\ g^{-1}$, which is slightly smaller than that of the monolith calcined at 900 °C, indicating that the thermal stability of the monoliths is fairly good. For the sample calcined at 1300 °C, although the specific surface area and pore volume are very small (due to phase transfer from θ-Al_2O_3 to α-Al_2O_3), the macroscopic shape and the macroporous structure maintain very well and the monolith presents a much higher mechanical strength. So, this sample should be a promising catalyst support. For this application, the specific surface area can be markedly improved by coating a layer of oxide, as proposed in our previous works [30, 31].

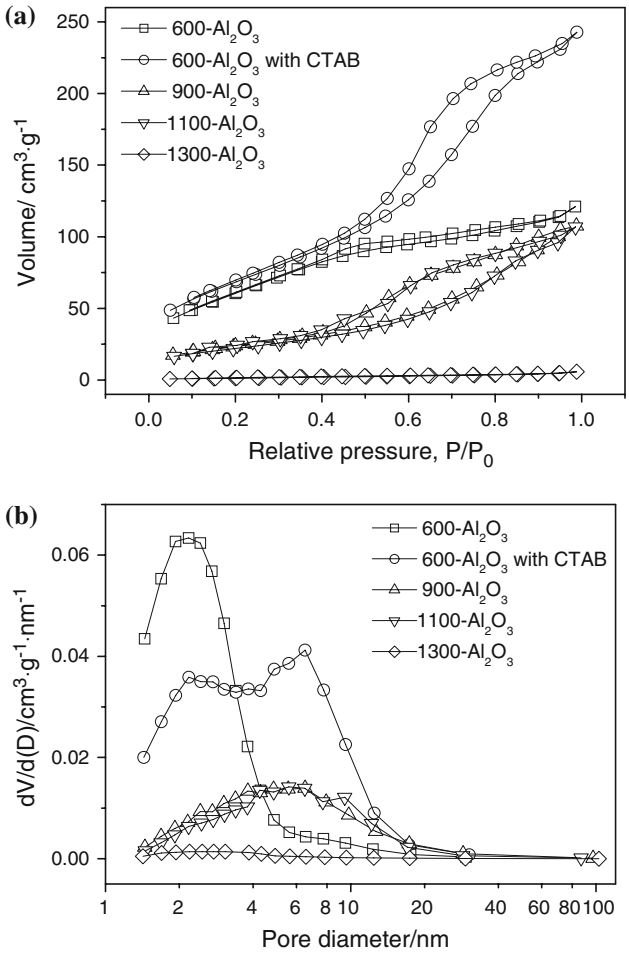

Fig. 6 N_2 adsorption–desorption isotherm and BJH pore size distribution curve of alumina monolith. **a** N_2 adsorption–desorption isotherms and **b** BJH pore size distribution curves

From Fig. 6a, the N_2 adsorption–desorption isotherm, all samples present a type II isotherm with the type B hysteresis loop (or type H3) [32]. In the preparation process of filling, the filling precursor, alumina hydrosol, was composed of colloid particles (in nano-sizes) suspended in the water. These nano-colloid particles packed together, forming meso(nano)-pores, resulting in this kind of isotherm. As shown in Fig. 6b, the monoliths are provided with micro/meso pores and the pore sizes are in the range of about 1 to 10 nm. The pore diameter increases with the increase of the calcination temperature, due to the sintering of the micropores. Comparing the adsorption–desorption isotherm of the 600 °C calcined sample with that of 900 °C and 1100 °C calcined samples, the latter two hystereses are much more evident. This hysteresis is due to the sintering of the small alumina particles at higher calcination temperatures. The TEM images in S4 of the supplementary information show that the size of the alumina particles increases with the increase in calcination temperature. The

microscopic morphology of the alumina particles calcined at different temperatures is similar with the results in the Ref. [33]. The sintering results in the changes of pore structure both in pore size and pore shape, giving hysteresis loops in the two isotherms.

The micro/mesoporous structure of the alumina monoliths can be modified and adjusted by adding surfactants. Adding surfactant CTAB into the alumina hydrosol leads to increase in both of the specific surface area and the pore volume of the alumina monolith (Table 1). The pore diameter of the meso-macroporous sample presents dual maxima in 2.2 nm and 6.5 nm, in which the pores in size of 6.5 nm are formed by the CTAB surfactant (as template), and the pore volume of the meso-macroporous sample is almost two times of the pore volume of the macroporous sample without CTAB.

Discussion

It is stated in the introduction section that as far as we know, no reports are found for preparing macroporous alumina monolith by using the template method. That the porous alumina monolith is hard to be prepared by polymer template method should be due to two reasons. First the alcosols of alumina precursor are hard to be made. Typical aluminum alkoxides such as aluminum tri-isopropoxide and aluminum tri-*sec*-butoxide have high viscosity and are very sensitive to water [22]. While for silica and titania, the corresponding solution and sol can be facilely made by just stirring the mixture of their alkoxide and alcohol (and surfactant for forming mesopores) at ambient temperature [10]. The second reason is that the organic polymer templates are usually hydrophobic, so filling the hydrophilic hydrosol into the templates is also a hard work. For the template method, one of the key steps is sol filling, while both alcosol and hydrosol seems nonapplicable, thus the template method seems not suitable for the porous alumina monolith preparation.

However, as mentioned above, alumina hydrosols are easy to be made and the residual surfactant on the surface can play an important role during the filling process. After drying, the templates should be hydrophilic or less hydrophobic, owing to the surfactant residues. Thus, the alumina hydrosol could be filled into the templates. That should be the reason for why alumina monolith can be fabricated from alumina hydrosol via such a template method.

At the same time, from the N_2 adsorption–desorption results, the walls of the so-prepared alumina monoliths are occupied with micro/meso pores. Combined with the SEM images (Fig. 6), the macroporous alumina monoliths take on a multi-level porous structure, that is to say, the monoliths are enriched with interconnected macropores with meso/micro pores spreading over the walls of the macropores.

The density, phase, and strength of the alumina monoliths are interrelated. The strength of the alumina monolith is obviously affected by the calcination temperature, as listed in Table 1. So, the strength can appropriately be enhanced by increasing the calcination temperature. The shrinkage increases with the increase of the calcination temperature (S2 in supplementary information). The higher shrinkage leads to the higher density of the monolith walls, and thus leads to the higher mechanical strength of the monoliths. On the other hand, as the calcination temperature increases, the structural transformation of the alumina occurred (Fig. 3). The phase of the alumina changes from γ-Al_2O_3 to θ-Al_2O_3, and finally to α-Al_2O_3 with the increase of the calcination temperature. The sintering of the alumina particles and the change of the crystal phase also influence the compressive strength.

The size of macropores in the monoliths can be controlled and adjusted by the porous structure of template and by calcination temperature of monolith to some extent. The meso/microporous structure of monolith can be adjusted by adding surfactant, such as CTAB in this work. Thus alumina monolith with hierarchical pore structure can be made by this template method and the pore structure is controllable.

The so-prepared alumina monolith with hierarchical porous structure should be a promising material. Using it as catalyst support is under work in our lab [2].

Conclusions

Macroporous monolith of alumina can be prepared by polymer template method. In this work, polystyrene foams were used as templates and alumina hydrosols were used as filling precursors, thus alumina monoliths with micro/meso-macroporous structure have been made. The hydrophilic hydrosol can be filled into the hydrophobic template foam, which is possibly owing to the residual surfactant introduced during template preparing process. This method used for preparing alumina monolith also possesses its advantages, such as monolith shape moldable and macroporous structure controllable. Moreover, by using this method, the meso/microporous structure of the alumina monolith can be adjusted by adding surfactants.

Acknowledgement The financial support of this work by Hi-tech Research and Development Program of China (863 program, Granted as No. 2006AA05Z115 and 2007AA05Z104) and the Cheung Kong Scholar Program for Innovative Teams of the Ministry of Education (No IRT0641) are gratefully acknowledged.

References

1. Vantomme A, Léonard A, Yuan ZY, Su BL (2007) Colloids Surf A Physicochem Eng Asp 300:70
2. Zhang Y, Zhao CY, Liang H, Liu Y Catal Lett. doi: 10.1007/s10562-008-9686-z
3. Liang C, Dai S, Guiochon G (2003) Anal Chem 75:4904
4. Bing Z, Yuan Y, Wang Y, Fu ZW (2006) Electrochem Solid State Lett 9:A101
5. Imhof A, Pine DJ (1997) Nature 389:948
6. Imhof A, Pine DJ (1998) Adv Mater 10:697
7. Stein A (2001) Microporous Mesoporous Mater 44–45:227
8. Stein A, Schroden RC (2001) Curr Opin Solid State Mater Sci 5:553
9. Guliants VV, Carreon MA, Lin YS (2004) J Memb Sci 235:53
10. Maekawa H, Esquena J, Bishop S, Solans C, Chmelka BF (2003) Adv Mater 15:591
11. Ma X, Sun H, Yu P (2008) J Mater Sci 43:887. doi:10.1007/s10853-007-2189-2
12. Li F, Wang Z, Ergang NS, Fyfe CA, Stein A (2007) Langmuir 23:3996
13. Ren J, Du ZJ, Zhang C, Li HQ (2006) Chin J Chem 24:955
14. Alvarez S, Esquena J, Solans C, Fuertes AB (2004) Adv Eng Mater 6:897
15. Lu AH, Smatt JH, Backlund S, Lindén M (2004) Microporous Mesoporous Mater 72:59
16. Tonanon N, Siyasukh A, Wareenin Y, Charinpanitkul T, Tanthapanichakoon W, Nishihara H, Mukai SR, Tamon H (2005) Carbon 43:2808
17. Zhang JC, Zhang H, Wu LB, Ding JD (2006) J Mater Sci 41:1725. doi:10.1007/s10853-006-2873-7
18. Bil M, Ryszkowska J, Kurzydłowski KJ J Mater Sci. doi: 10.1007/s10853-008-3037-8
19. Sánchez-Valente J, Bokhimi X, Hernández F (2003) Langmuir 19:3583
20. Kasprzyk-Hordern B (2004) Adv Colloid Interface Sci 110:19
21. Pesek JJ, Matyska MT (2002) J Chromatogr A 952:1
22. Tokudome Y, Fujita K, Nakanishi K, Miura K, Hirao K (2007) Chem Mater 19:3393
23. Fujita K, Tokudome Y, Nakanishi K, Miura K, Hirao K (2008) J Non Cryst Solids 354:659
24. Murai S, Fujita K, Nakanishi K, Hirao K (2006) J Alloys Compd 408–412:831
25. Han YS, Li JB, Chen YJ (2003) Mater Res Bull 38:373
26. Han YS, Li JB, Wei QM, Tang K (2002) Ceram Int 28:755
27. Zhao S, Zhang J, Weng D, Wu X (2003) Surf Coat Tech 167:97
28. Levin I, Brandon D (1998) J Am Ceram Soc 81:1995
29. Chin P, Sun X, Roberts GW, Spivey JJ (2006) Appl Catal A Gen 302:22
30. Zeng SH, Liu Y, Wang YQ (2007) Catal Lett 117:119
31. Zeng SH, Liu Y (2008) Appl Surf Sci 254:4879
32. Gregg SJ, Sing KSW (1982) Adsorption, surface area and porosity. Academic Press, London, p 304
33. Santons HS, Kiyohara PK, Santos PS (1994) Ceram Int 20:175